Arch. Metall. Mater. **65** (2020), 3, 989-992

DOI: 10.24425/amm.2020.133203

HYEONDEOK JEONG[1], SUNG-SOO RYU[1*]

EFFECT OF GLASS-COATED Al PASTE ON BACK-SURFACE FIELD FORMATION IN Si SOLAR CELLS

In this study, glass frit was coated uniformly on the surface of Al particles instead of adding glass frit to Al powder by simple mixing to form a nano-layer. The influence of the glass-frit coating on the formation of the back-surface field and electrical characteristics of the resulting Al electrode were investigated. Microstructural observations indicated that the glass components were uniformly distributed and the back-surface field layer thickness was more uniform compared to the simply mixed sample. In addition, the sheet resistance was <10 mΩ/□, much lower than the 23 mΩ/□ of the simply mixed Al electrode.

Keywords: Si solar cell, Al paste, glass coating, Al back contact, back-surface field

1. Introduction

Al thick films are widely used as backside contacts in single-crystalline and polycrystalline Si solar cells. Al electrodes are commonly prepared by the firing of previously screen-printed layers and the electrodes are formed using a paste containing Al powder as well as inorganic and resin binders [1-4]. Pb-based glass frits exhibit superior sintering characteristics and have conventionally been used as inorganic binders [5]. However, there are various researches have been tried to develop Pb-free glass frits as well, since Pb is not environmentally-friendly [6-8]. Al electrodes formed by firing at high temperatures serve as electrical contacts and Al is also used to produce a back-surface field (BSF) [9,10]. In these materials, a thick Al layer is alloyed with silicon during contact firing, allowing the BSF to reduce back-surface recombination and increase solar cell efficiency.

Glass provides adhesion strength in Si cells and increases Al particle sintering as an inorganic binder by liquid phase sintering [11]. However, it negatively affects the electrical properties of Si cells because of its inherent insulation characteristics. The size, shape, and composition of the glass particles and mixing state between glass and Al particles are important parameters that can impact cell performance [12,13]. Generally, glass particles are mixed with Al powder by simple mixing, which may cause inhomogeneity between the Al and glass in Al paste, resulting in glass aggregation after sintering. Therefore, glass phase uniformity is very important for improved cell efficiency [14-16]. The refinement of glass particle size, spherical glass particle shape, and/or homogenous distribution of glass particles can improve cell performance.

Herein, glass was coated on Al particles to improve the mixing degree between Al and glass. The glass-coated Al (GCA) is expected to behave differently during sintering compared to conventional glass-mixed Al (GMA). An Al paste was developed using glass-coated Al powder to produce back contacts for Si solar cells. The B-Bi-Si-O composition of the glass phase as an inorganic additive was coated on Al to achieve this objective. The electrical resistance of the Al electrode and corresponding cell performances were investigated and compared to those prepared by conventional mixing.

2. Experimental

The glass-coating process on the Al powder was performed by spray pyrolysis using a water-based B-Bi-Si solution. B-Bi-Si solution was prepared by dissolving ammonia borane (H_3NBH_3), bismuth nitrate ($Bi(NO_3)_3 \cdot 5H_2O$) and TEOS ($C_8H_{20}O4Si$) in sequence with a mixing time of 10 min for each element into a distilled water, followed by spray pyrolysis processing at 150°C. After coating, the Al powder was calcined at 300°C for 1 h under an Ar atmosphere to prevent oxidation. The glass-coated Al powder was then dispersed in an organic binder mixture with a 3-roll mill to produce a screen-printable Al paste. For com-

[1] KOREA INSTITUTE OF CERAMIC ENGINEERING AND TECHNOLOGY, ENGINEERING CERAMIC CENTER, GYEONGCHUNG-DAERO 3321, SINDUN-MYEON, ICHEON-SI, GYEONGGI 17303, REPUBLIC OF KOREA

* Corresponding author: ssryu@kicet.re.kr

parison with the glass-mixed Al electrode, a paste was prepared by simple mixing of Al and 2 wt% glass powder by the same process described above. Fig. 1 shows a schematic diagram of the glass-coated and glass-mixed Al powder preparation and corresponding sintering behaviors.

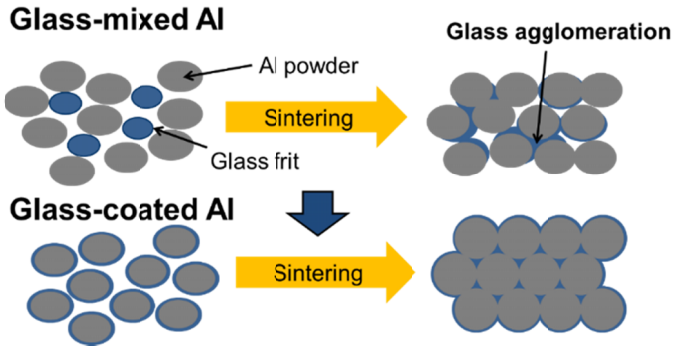

Fig. 1. Schematic diagram of glass-mixed and glass-coated Al powder sintering behaviors

Screen-printed solar cells (15.6 cm^2) were fabricated on monocrystalline p-type Si wafers using the carefully fabricated Al pastes in an infrared (IR) belt furnace. The Si wafers were chemically cleaned and wet-etched and subsequently diffused with $POCl_3$ in a tube furnace to form a high-sheet-resistance n+ emitter. After the phosphorus glass was removed from the emitter by a second cleaning with hydrofluoric acid, plasma enhanced chemical vapor deposition (PECVD) was used to deposit a SiN_x antireflective coating onto the emitter. One of the three Al pastes was subsequently screen-printed onto the back side of the Si wafers and the wafers were oven dried at 230°C for 10 min. Ag grids were then screen-printed on top of the SiN_x coating layer and oven dried at 230°C for 10 min. The Ag and Al contacts were cofired at 800°C in an IR lamp-heated, five-zone, belt-line furnace. The cells were fired at 800°C, which was the peak temperature measured in the furnace atmosphere, corresponding to a belt speed of 600 mm/s operated for 60 s.

The finished cells were characterized via I-V analysis under the standard operating conditions of AM 1.5 (1000 Wm^{-2}) irradiance. The cell efficiency was determined using this test and electrical sheet resistance was measured using the 4-point probe method. Scanning electron microscopy (SEM; JSM-6360LV, JEOL, Japan) was performed to identify the Al-Si reaction layer and the samples were etched in a 1:2:3 vol/vol solution of HF-HNO_3-H_2O (deionized water) for 15 s.

3. Results and discussion

Fig. 2 shows a TEM micrograph and the TEM-EDS results of the glass-coated Al powders. As shown in Fig. 2a, the Al particle size was sub-micron and an approximately 20 nm thick glass layer was formed on the Al particle surface. The point EDS results of the coating layer indicated the presence of Bi, Si, and O, which are common components of glass, while B was not detect by EDX due to its low mass.

Fig. 3 shows the cross-sectional back-scattered SEM images of the back side of the GCA electrodes as a function of sintering temperature. The Al layer, Al-Si eutectic layer, heavily p-doped P+ region (BSF layer), and Si substrate were observed after sintering at 700°C, becoming clearer with increasing sintering temperature. BSF layer thickness also increased with increasing sintering temperature up to 800°C and no further change occurred after 900°C. This SEM analysis showed that the BSF layer was well established using the GC Al paste and sintering at 800°C.

Fig. 4 shows the cross-sectional back-scattered SEM images of the back side of the GMA and GCA electrodes. The Al layer, Al-Si eutectic layer, heavily p-doped P+ region, and Si substrate were clearly observed in both specimens. However, the BSF layer thickness in the GCA electrode was 6-7 μm, higher than that of GMA electrode (4-5 μm) due to glass dispersion in the Al particles.

Fig. 5 shows SEM images of the surface morphologies of the screen-printed Al back contacts prepared with GMA and GCA pastes after firing at 800°C. Dense microstructures were observed in both sample regardless of the glass-addition process. However, white regions representing agglomeration of the glass phases were observed in the sample prepared with the GMA

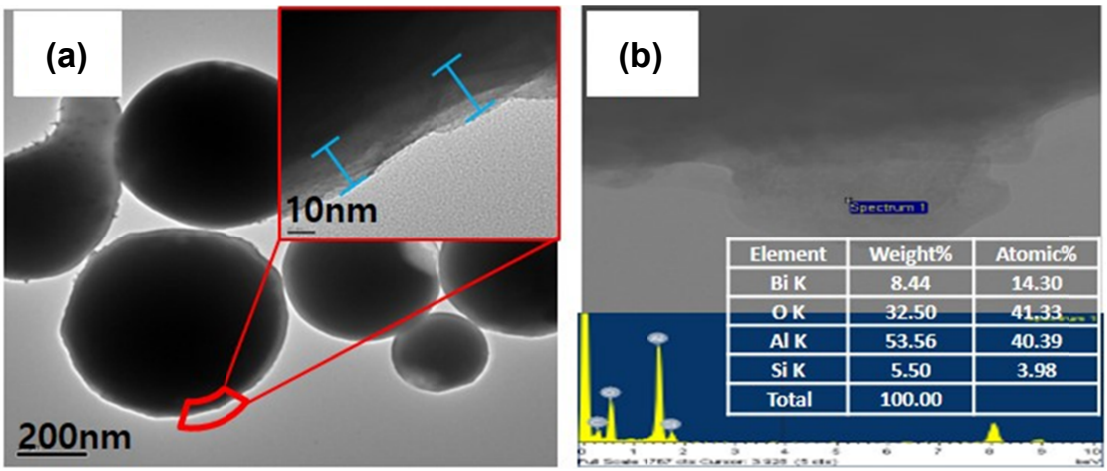

Fig. 2. (a) TEM micrograph and (b) TEM-EDS results of the glass-coated Al powders

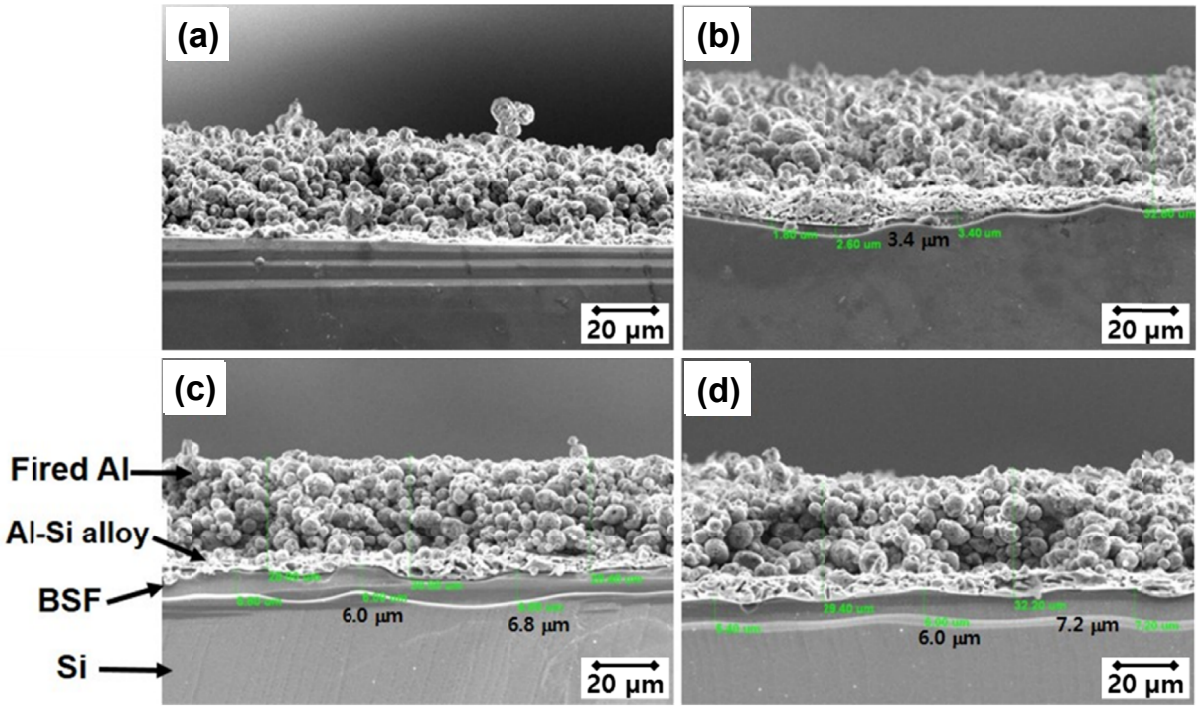

Fig. 3. Cross-sectional back scattered SEM images showing changes in the BSF layer thickness of back contacts produced using the glass-coated Al paste as a function of sintering temperature: (a) 600°C, (b) 700°C, (c) 800°C, (d) 900°C

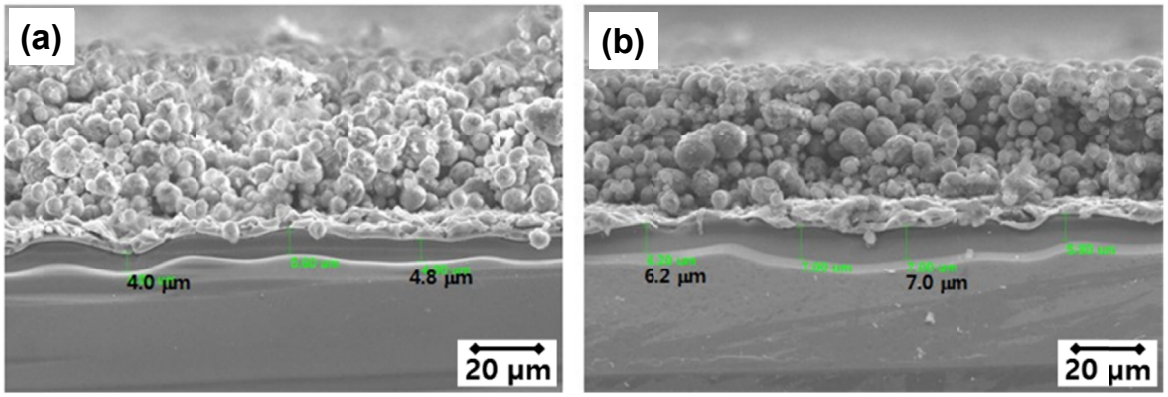

Fig. 4. Cross-sectional back scattered SEM images showing changes in the BSF layer thickness of back contacts produced using the (a) glass-mixed and (b) glass-coated Al pastes which fired at 800°C

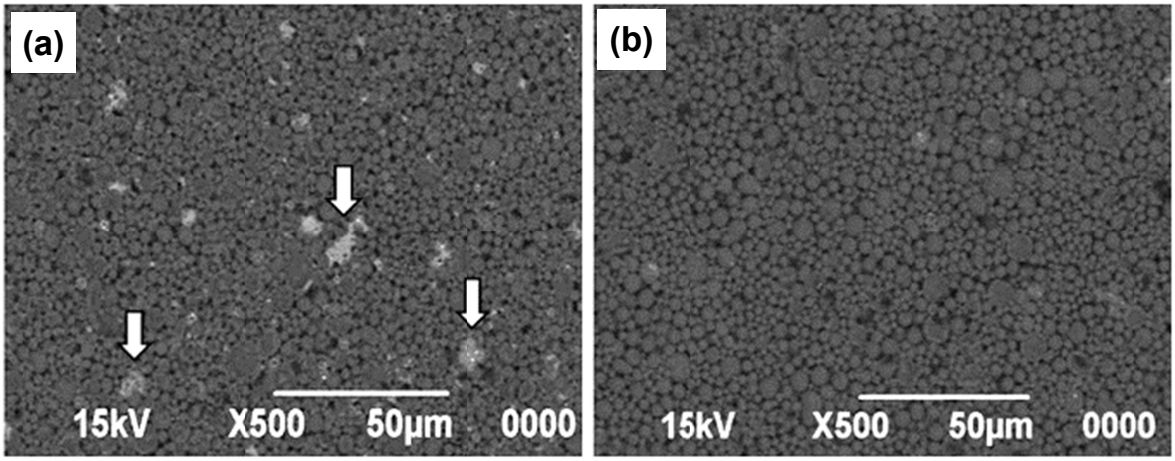

Fig. 5. SEM images of the surface morphologies of back contacts screen-printed using the (a) glass-mixed and (b) glass-coated Al pastes fired at 800°C

paste (Fig. 5a). For the GCA sample, the glass phase was well dispersed between Al particles (Fig. 5b), suggesting that the glass-coating process can improve the degree of distribution of the glass phase in the Al electrode. Adding a glass frit binder to the Al electrode increases the contact between Al particles, and a good connectivity between Al particles is required for fabricating electrodes with good electrical conductivity, i.e., lower electrical resistance. Therefore, if the connections between Al particles are hindered by glass agglomeration, the electrical sheet resistance could be deteriorated.

The electrical sheet resistances of GMA and GCA pastes after sintering at 800°C were compared and the results are shown in Fig. 6. The sheet resistance of the GCA paste was <10 mΩ/□, much lower than the 23 mΩ/□ obtained for the GMA paste. The reason of higher sheet resistance for GMA than GCA is estimated the agglomeration and defect formation of as shown in Fig. 5.

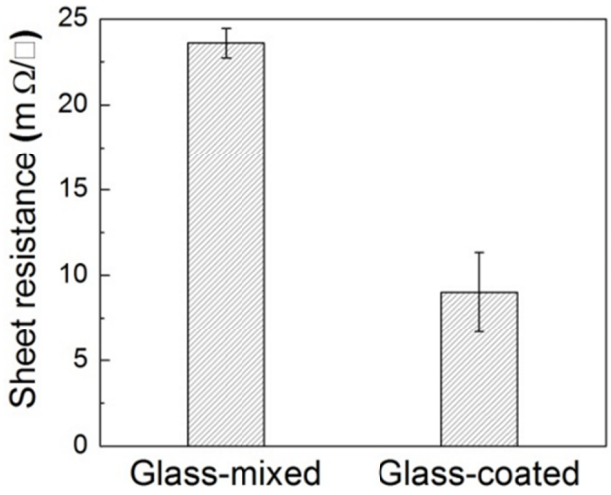

Fig. 6. Comparison of the glass-mixed and glass-coated Al electrodes in terms of electrical sheet resistance after sintering at 800°C

Table 1 shows the electrical characteristics of the Al-BSF Si solar cells produced using the GMA and GCA pastes. The GCA sample exhibited a higher open-circuit voltage (Voc) and fill factor (FF) than the sample prepared with GMA. As previously mentioned, the Al-BSF layer, which is uniform and thick, is important for preventing the recombination of electron holes on the back sides of Si cells [1,2] and increases the passivation effect and solar cell efficiency. This can cause increased Voc and FF, increasing the conversion efficiency of the resulting Si cells. This can be attributed to the more uniform BSF layer and homogeneous glass phase distribution, as was observed using SEM imaging, as well as the good conductivity of the Al paste, leading to the higher cell efficiency.

TABLE 1

Electrical characteristics of the Al-BSF Si solar cells prepared with glass-mixed and glass-coated Al electrodes

Al Paste	Efficiency (%)	Fill factor (%)	Voc (mV)	Isc (A)	Jsc (A/cm^2)
Glass-mixed	12.0	58.0	565.6	4.0	35.1
Glass-coated	13.0	65.2	585.8	3.4	34.1

4. Conclusions

The prepared 1 wt% B_2O_3-ZnO-SiO_2 glass was coated on Al particle surfaces to form a nano-layer. The glass coating was uniformly distributed and produced a uniform BSF layer compared with the glass-mixed sample. In addition, the sheet resistance of the glass-coated sample was <10 mΩ/□, much lower than the 23 mΩ/□ of the simply mixed Al electrode.

Acknowledgments

This work was supported by Korea Institute of ceramics Engineering and Technology.

REFERENCES

[1] S. Kim, S. Sridharan, C. Khadilkar, A. Shaikh, Conference Record of the Thirty-first IEEE Photovoltaic Specialists Conference, 1100 (2005).
[2] H.-C. Fang, C.-P. Liu, H.-S. Chung, C.-L. Huang, J. Electrochem. Soc. **157**, H455 (2010).
[3] M. Balucani, L. Serenelli, K. Kholostov, P. Nenzi, M. Miliciani, F. Mura, M. Izzi, M. Tucci, Energy Procedia **43**, 100 (2013).
[4] K.H. Kim, C.S. Park, J.D. Lee, J.Y. Lim, J.M. Yeon, I.H. Kim, E.J. Lee, Y.H. Cho, Jpn. J. Appl. Phys. **56**, 08MB25 (2017).
[5] J. Yi, H. Koo, J.H. Kim, Y. Ko, Y. Kang, H.M. Lee, J. Yun, J. Alloys Compd. **490**, 488 (2010).
[6] Q. Che, H. Yang, L. Lu, Y. Wang, Appl. Energy **112**, 657 (2013).
[7] J. Jiang, Y. He, Z. Zhang, J. Wei, L. Li, J. Alloy Compd. **689**, 662 (2016).
[8] W.-H. Lee, T.-K. Lee, C.-Y. Lo, J. Alloy Compd. **686**, 339 (2016).
[9] A. Kaminski, B. Vandelle, A. Fave, J.P. Boyeaux, L.Q. Nam, R. Monna, D. Sarti, A. Laugier, Sol. Energy Mater. Sol. Cells **72**, 373 (2002).
[10] N. Chen, A. Ebong, Sol. Energy Mater. Sol. Cells **146**, 107 (2016).
[11] R.M. German, P. Suri, S.J. Park, J. Mater. Sci. **44**, 1 (2009).
[12] J.H. Yi, J.H. Kim, Y.N. Ko, Y.J. Hong, H.Y. Koo, Y.C. Kang, H.M. Lee, J. Ceram. Soc. Jpn. **119**, 954 (2011).
[13] J. Zhou, X. Chen, Y. Wang, B. Zhao, Mater. Lett. **169**, 197 (2016).
[14] S. Yuan, Y. Chen, Z. Mei, M.-J. Zhang, Z. Gao, X. Wang, X. Jiang, F. Pan, Chem. Commun. **53**, 6239 (2017).
[15] Y. Kim, J. Huh, H. Kim, Sol. Energy Mater. Sol. Cells **185**, 97 (2018).
[16] J. Zhang, H. Li, H. Tong, S. Xiong, Y. Yang, X. Yuan, H. Li, C. Liu, Appl. Sci. **9**, 891 (2019).